



저작자표시-비영리-변경금지 2.0 대한민국

이용자는 아래의 조건을 따르는 경우에 한하여 자유롭게

- 이 저작물을 복제, 배포, 전송, 전시, 공연 및 방송할 수 있습니다.

다음과 같은 조건을 따라야 합니다:



저작자표시. 귀하는 원저작자를 표시하여야 합니다.



비영리. 귀하는 이 저작물을 영리 목적으로 이용할 수 없습니다.



변경금지. 귀하는 이 저작물을 개작, 변형 또는 가공할 수 없습니다.

- 귀하는, 이 저작물의 재이용이나 배포의 경우, 이 저작물에 적용된 이용허락조건을 명확하게 나타내어야 합니다.
- 저작권자로부터 별도의 허가를 받으면 이러한 조건들은 적용되지 않습니다.

저작권법에 따른 이용자의 권리는 위의 내용에 의하여 영향을 받지 않습니다.

이것은 [이용허락규약\(Legal Code\)](#)을 이해하기 쉽게 요약한 것입니다.

[Disclaimer](#)

Doctor of Philosophy

Validation and Comparison of Collagenase Induced and Window

Defect Achilles Tendon Injury Model in Rats

The Graduate School
of the University of Ulsan
Department of Medicine

JaYoung Kim

Validation and Comparison of Collagenase Induced and Window
Defect Achilles Tendon Injury Model in Rats

Supervisor: KyoungHyo Choi

A Dissertation

Submitted to
the Graduate School of the University of Ulsan
In partial Fulfillment of the Requirements
for the Degree of
Doctor of Science
by
JaYoung Kim

Department of Medicine
Ulsan, Korea
February 2021

Validation and Comparison of Collagenase Induced and Window
Defect Achilles Tendon Injury Model in Rats

This certifies that the dissertation of JaYoung Kim is approved.

Committee Chair: Dr. Jae Yong Jeon _____

Committee Member: Dr. Kyoung Hyo Choi _____

Committee Member: Dr. Dae Yul Kim _____

Committee Member: Dr. Won Kim _____

Committee Member: Dr. Seoyon Yang _____

Department of Medicine

Ulsan, Korea

February 2021

ABSTRACT

Objective Selecting an appropriate animal model is important for animal studies. The objective of the study was to validate and compare rat collagenase induced Achilles tendon injury models and rat window defect induced Achilles tendon injury models.

Method Fifty-four Achilles tendons from twenty-seven 10-week-old male Sprague Dawley rats were randomly assigned to three groups: (1) collagenase group; (2) window defect group; and (3) normal control group. Ten microliters of type I collagenase double injection was administered to the Achilles tendon of the collagenase group. A defect (0.6 mm × 6 mm) was generated at the tendon insertion site of the calcaneus of the window defect group. Cross-sectional areas (CSAs), biomechanical properties, and histological characteristics were assessed at 2 and 4 weeks following each tendon injury.

Results The CSAs in both collagenase and window defect groups increased at 2 weeks, but decreased at 4 weeks. CSAs of both injury models were significantly larger than those of the normal group at both 2 and 4 weeks. CSAs of the collagenase group were significantly larger than those of the window defect group at 4 weeks. Biomechanical properties of both injury models decreased at 2 weeks and increased at 4 weeks. Ultimate failure load, stiffness, and maximal stress of both groups were significantly lower than those of the normal group at 2 weeks. At 4 weeks, ultimate failure load and stiffness in the collagenase group were not significantly lower than those in the normal group. Both models displayed diffuse tendinopathy in all H & E stained slides. Modified Watkins scores in the window defect group

were significantly lower than those in the collagenase group at 4 weeks. Chondrocyte-like cells and lacunae were found in both groups at both time points. There were no intergroup differences in the compositions of collagen type I, collagen type III, tenascin C and BMP 2.

Conclusion Both collagenase and window defect-induced rat Achilles tendon injury models are suitable for tendon injury studies. Although there was no marked difference between these two models, the window defect model showed a tendency towards slower recovery.

Key Word: Models, Animal, Rats, Achilles tendon, Collagenase

Contents

Abstract	i
Contents	iii
Lists of tables	iv
Lists of figures	v
Introduction	1
Methods	2
Results	7
Discussion	14
Conclusion	17
References	17
Abstract (Korean)	21

Lists of tables

Table 1. Modified Watkin score 6

Lists of figures

Fig. 1. Flowchart of this study	3
Fig. 2. Generating the window defect on Achilles tendon	4
Fig. 3. Cross-sectional areas of tendons in each group	8
Fig. 4. Biomechanical properties of tendons in each group	9
Fig. 5. Modified Watkins scores of tendons in each group	10
Fig. 6. Hematoxylin and eosin staining	11
Fig. 7. Representative images of chondrocyte-like cells, lacunae	12
Fig. 8. Quantification of 4 proteins by immunohistochemistry	13
Fig. 9. Quantification of 4 proteins by western blot	14

INTRODUCTION

Prevalence of tendon injuries impacts the ability to exercise and work [1]. Because tendons display poor healing abilities, there is a constant demand for better treatments for tendon injuries. Appropriate animal tendon injury models are necessary not only for understanding the physiological processes underlying tendon injury and repair, but also for evaluating the effects of various treatments [2, 3]. Rats have often been used to model tendon injuries, with particular reference to chemically- or mechanically-induced models of tendinopathy [2]. *In vivo* studies pertaining to stem cell therapy of tendon injuries using rat Achilles tendon models involve either collagenase-induced lesions or surgical transections [4-8].

A collagenase-induced tendon injury model is usually constructed by administering a type I collagenase injection to the tendon. This method involves catalyzing the breakdown of collagen type I, the most abundant extracellular matrix component of the tendon which constitutes almost 60% of the dry mass of the tissue and approximately 95% of the total collagen [9]. Progressive tendon reparation takes place following an acute and intense inflammatory reaction caused by an intratendinous collagenase injection [10, 11]. The rate of recovery is one of the determining factors for selecting an animal model. Although one study has discussed the collagenase-induced natural healing process in rat Achilles tendon injury models studies comparing the rates of recovery of different models are scarce [12].

Detailed techniques used by these studies to perform surgical transections were somewhat different. Huang and Okamoto made a cut in the Achilles tendon, whereas Lee and Yang made a rectangular defect at the Achilles tendon of rats [5-7, 13]. A rectangular defect, also known as a window defect, is more often used in rat patellar tendon injury models [14-16]. The common feature of studies that used window defects in rat tendons was that these investigated stem cell intervention. However, studies that validate window defect tendon injury models are yet to be conducted.

Animal studies using rat Achilles tendon injury models are conducted frequently. Use of a valid animal model increases confidence in the results of any study investigating tendon injuries. Some previous

studies evaluated rat Achilles tendon injury models generated by repetitive muscle exercise in a kicking machine or by administering peritendinous injections of prostaglandin E1 [17, 18]. Perucca evaluated rat Achilles tendon collagenase models histologically, but did not assess biomechanical properties, which are considered to be an important element of any tendon study [19].

Currently, there is a lack of studies comparing different types of rat Achilles tendon injury models. Animal tendon injury models generated using different methods may display different characteristics. For instance, the rate of recovery, calcification, and the degree of variability in each model may show differences. These data may enable researchers designing animal studies to investigate tendon injuries to select appropriate animal models according to their objectives. For example, a researcher investigating calcific tendinitis may attempt to select an animal model that best reveals calcification.

Of the many different types of animal tendon injury models that were available, the collagenase-induced and window defect-induced tendon injury models were selected for evaluation. The objective of the present study was to validate rat collagenase-induced and rat window defect-induced Achilles tendon injury models. I evaluated histopathological and biomechanical properties, both of which are recognized as features associated with tendinopathy in humans [20]. In addition, I aimed to determine the characteristics that differed between these two models.

METHODS

1. Study Design

A total of 54 Achilles tendons from twenty-seven 10-week-old male Sprague Dawley rats (Orient Bio, Seongnam, Korea) were used. Eighteen tendons were randomly divided into three groups as follows: (1) the collagenase group; (2) the window defect group; and (3) the normal control group. Outcome parameters such as the cross-sectional area (CSA), biomechanical properties and histological characteristics, as well as the results of immunohistochemistry (IHC) and western blot analyses, were assessed at 2 and 4 weeks following each tendon injury. Six tendons were used to assess each parameter

at each time point except for CSA, which was assessed using 18 tendons. A schematic of the study design is shown (Fig. 1). All study procedures were approved by the Institutional Animal Care and Use Committee of Asan Medical Center, Asan Institute for Life Sciences (IACUC Approval No.: 2018-12-006).

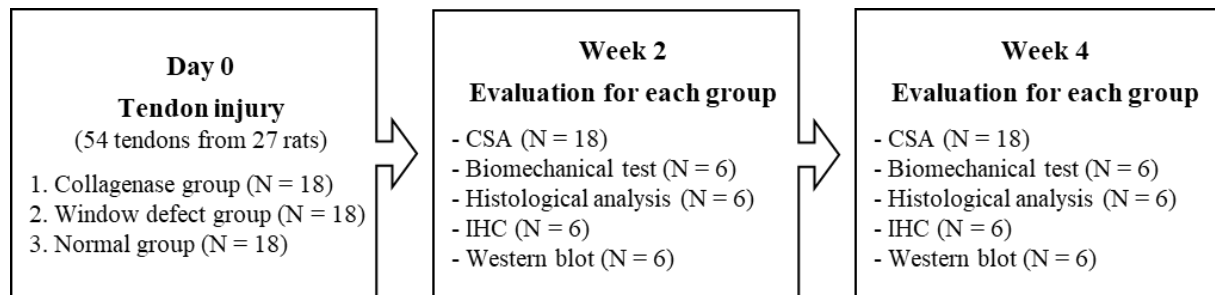


Fig. 1. Flowchart of this study.

N, number of tendons; CSA, cross sectional area; IHC, immunohistochemistry

CSA, biomechanical test, histological analysis was performed for all three groups. IHC and western blot were conducted only in collagenase and window defect groups.

2. Surgical Procedure

Surgical procedures were performed while the rats were anesthetized with 2% isoflurane. An approximately 15-mm longitudinal skin incision was made over the Achilles tendon using micro-scissors. After the tendon was exposed, a 10 μ L type I collagenase (62.5 IU/10 μ L) double injection (10 μ L for each tendon strip, for a total of 20 μ L with 125 IU) was administered to each rat Achilles tendon of the collagenase group. In the window defect group, a 0.6 mm wide and 6 mm long defect was made at the tendon insertion site of each calcaneus, using two No. 11 surgical blades and a custom-made plastic rack assembly created using a 3D printer (Fig. 2); [6]. After removing the central tendon tissue between the incisions, a standardized window defect of the Achilles tendon was made. These defects were made in both hind limbs and the skin was closed with non-absorbable 4-0 silk sutures. The activity of the rats was not restricted during the study.



Fig. 2. Generating the window defect on Achilles tendon

3. CSA measurements

Tendons were harvested at 2 and 4 weeks after model formation (18 tendons each for normal, collagenase, window defect group at 2 and 4 weeks), and the rats were euthanized via carbon dioxide inhalation. The width and depth of all tendons were measured at the midpoint of the Achilles tendon, using a digital caliper (ULJ-15; Nakamura Mfg. Co., Ltd., China). Assuming that the cross-section of a tendon is elliptical, tendon CSA was calculated as $CSA = \pi \times \text{width} \times \text{depth}/4$ [21, 22]. Thickness was measured thrice in order to reduce measurement error and the median value was used for calculations.

4. Biomechanical Test

For the biomechanical test, tendons ($n = 6$ tendons for normal, collagenase and window defect groups at 2 and 4 weeks) were harvested while still attached to the foot, and the calf muscle was transected through the muscle belly. The tendon-foot complexes were stored at -80°C to prevent tissue damage. Prior to the test, the tissues were thawed at room temperature and calf muscle around the tendon was trimmed using micro-scissors.

The distal end around the proximal metatarsal bone was press-fixed in a metallic clamp. The tendon at 5 mm from the Achilles tendon insertion site was fixed using a custom-made tendon clamp. The tendons were mounted on a biomechanical testing machine (JSV-H100; JISC, Tokyo, Japan) with a 100-N load

cell. The construct was initially set to a basic axial stress of 0.1 N preload for straightening. Each tendon was then axially pulled at a constant speed of 10 mm/min until ultimate failure load was reached [6]. Ultimate failure load (N), stiffness (N/mm; from each tendon's stress-strain curve) and maximal stress (N/mm² = ultimate failure load/CSA) were measured [23]. Higher values of each of the three indicators were regarded as indicators of a healthier tendon.

5. Tissue Preparation and Histological Analysis

For histological analyses and IHC, the Achilles tendons were harvested between the calcaneus and the musculotendinous junction. Tissues were fixed in 4% paraformaldehyde for 5 d and rinsed with tap water for approximately 2 h. Next, the tissues were dehydrated in a graded ethanol series and cleared in xylene using a tissue processor (Shandon, Excelsior ES; Thermo Scientific, Rockford IL, USA). The tissues were then embedded in paraffin blocks, cut into 3 µm coronal sections, and stained with hematoxylin and eosin (H & E) using an automatic stainer (Leica autostainer, XL). Stained tissue slides were captured using a slide scanner (Pannoramic 250 Flash III; 3DHistech, Ltd., Budapest, Hungary). The captured slides were evaluated with a digital microscope application (CaseViewer version:2.2; 3DHISTECH Ltd., Hungary) in a blinded manner.

The modified Watkins score was used in order to quantitatively evaluate parameters of tendon histopathology [24, 25]. This scale consisted of 6 parameters as follows: cellularity, tenocytes, parallel cell orientation, vascularity, fiber diameter, and parallel fibers orientation. These were considered as characteristics indicating the maturity of cellular and intercellular constituents (Table 1) [24]. Each parameter was scored from 1 to 4, leading to a total score ranging from 6 to 24, where a lower score indicated a more degenerated tendon. This scoring system provided definitive quantitative criteria, where each criterion was presented as a percentage of mature tendon characteristics. In addition, I qualitatively evaluated chondrocyte-like cells, lacunae, and calcific deposits to determine ectopic chondrogenesis and ossification in the distal 1/3rd of the tendons.

Table 1. Modified Watkin score

	1	2	3	4
Cellularity	Marked	Moderate	Mild	Minimal
Tenocytes	<25%	25-50%	50-75%	>75%
Cells oriented parallel	<25%	25-50%	50-75%	>75%
Vascularity	>15 bv/low PF	11-15 bv/low PF	6-10 bv/low PF	<6 bv/low PF
Fiber diameter	<25%	25-50%	50-75%	>75%
Fibers oriented parallel	<25%	25-50%	50-75%	>75%

bv, blood vessel; PF, power field

6. Immunohistochemistry

The distributions of collagen type I, collagen type III, tenascin C and BMP 2 were assessed using an immunohistochemical staining test (n = 6 tendons, for normal, collagenase, and window defect groups at 2 and 4 weeks). The sections were immunolabeled with anti-collagen I (1:250 dilution; ab34710, Abcam), anti-collagen III (1:600; ab7778, Abcam), anti-tenascin C (1:8000; ab108930, Abcam) and anti-BMP2 (1:600; ab6285, Abcam) antibodies. Stained tissue slides were also captured using a slide scanner and evaluated via a digital microscope application. The relative stained area fraction for each antibody in the distal 1/3rd of the tendons was quantitatively evaluated using ImageJ (National Institutes of Health, Bethesda, MD, USA; <http://rsb.info.nih.gov/ij/>).

7. Tissue Preparation and Western Blot Analysis

For western blot analysis, the Achilles tendons were harvested between the calcaneus and the proximal tendon without muscle tissue (n = 6 tendons, for collagenase and window defect group at 2 and 4 weeks). Tendon tissues were frozen in liquid nitrogen and ground to a powder using a mortar and pestle. Subsequently, the ground tissues were digested in a buffer containing 8 M urea, 50 mM Tris-HCl at pH 8.0, 1 mM dithiothreitol, and 1 mM EDTA. Ten micrograms of extracted proteins were separated on 8–15% sodium dodecyl sulfate–polyacrylamide gels, transferred to polyvinylidene fluoride membranes (Bio-Rad, Hercules, CA, USA), blocked, and incubated at room temperature for 1 h 30 min. Next, the membranes were incubated at 4°C overnight with anti-collagen I (ab34710, Abcam), anti-collagen III

(ab7778, Abcam), anti-tenascin C (ab108930, Abcam) and anti-BMP2 (ab6285, Abcam) antibodies. β -actin (ab8227; Abcam) was used as an internal control. The membranes were washed for 10 min, five times, following incubation with a horseradish peroxidase-conjugated secondary antibody (1:3000 dilution) at room temperature for 90 min. Bands were visualized via ECL prime solution (Thermo Scientific). The intensity of the protein band was measured using Image J software (NIH).

8. Statistical Analysis

Differences between the two groups were analyzed using the Mann-Whitney U test, because the sample size of each variable was not large enough. Data were recorded and analyzed using PASW Statistics for Windows, version 18.0 (SPSS Inc., Chicago, IL, USA). Statistical significance was set at $p < 0.05$.

RESULTS

1. CSA of the tendon

CSAs of both collagenase and window defect groups were significantly larger than those of the normal group at 2 and 4 weeks (Fig. 3). Mean CSAs at 4 weeks were significantly smaller than those at 2 weeks in both collagenase ($14.75 \pm 3.81 \text{ mm}^2$ at 2 weeks vs $8.93 \pm 3.35 \text{ mm}^2$ at 4 weeks; $p < 0.001$) and window defect (13.82 ± 4.37 vs $5.96 \pm 1.84 \text{ mm}^2$; $p < 0.001$) groups. Although CSAs did not differ between the collagenase and window defect groups at 2 weeks ($p = 0.443$), the CSA of the window defect group was significantly smaller than that of the collagenase group ($p = 0.008$) at 4 weeks. The standard deviation of the collagenase group (3.35) was higher than that of the window defect group (1.84) at 4 weeks.

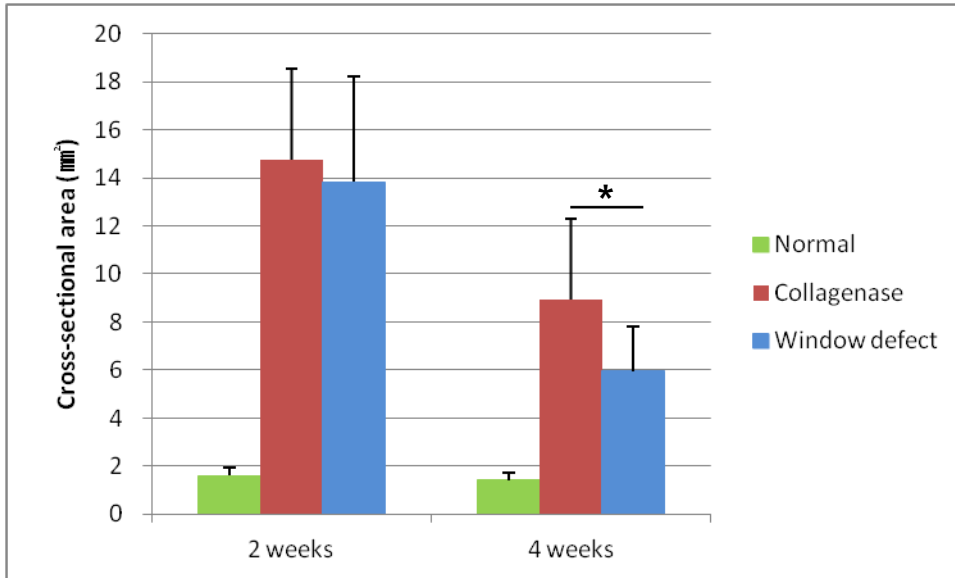


Fig. 3. Cross-sectional areas of tendons in each group.

* $p < .05$, between collagenase and window defect groups at 4 weeks; Mann-Whitney U test.

2. Biomechanical Test

Ultimate failure load, stiffness, and maximal stress of both collagenase and window defect groups were all significantly lower than those of the normal group at 2 weeks (ultimate failure load, $p = 0.009$ in collagenase and $p = 0.002$ in window defect group; stiffness, $p = 0.002$ in both group; maximal stress, $p = 0.002$ in both group); (Fig. 4). Although ultimate failure load and stiffness in the collagenase group were still lower than those of the normal group at 4 weeks, the difference was not statistically significant (ultimate failure load, $p = 0.093$; stiffness, $p = 0.394$; maximal stress, $p = 0.002$). All three biomechanical properties of the window defect group remained significantly lower than those of the normal group at 4 weeks (ultimate failure load, $p = 0.041$; stiffness, $p = 0.009$; maximal stress, $p = 0.002$). However, no significant differences were found between all biomechanical properties of the collagenase and window defect groups at 2 or 4 weeks.

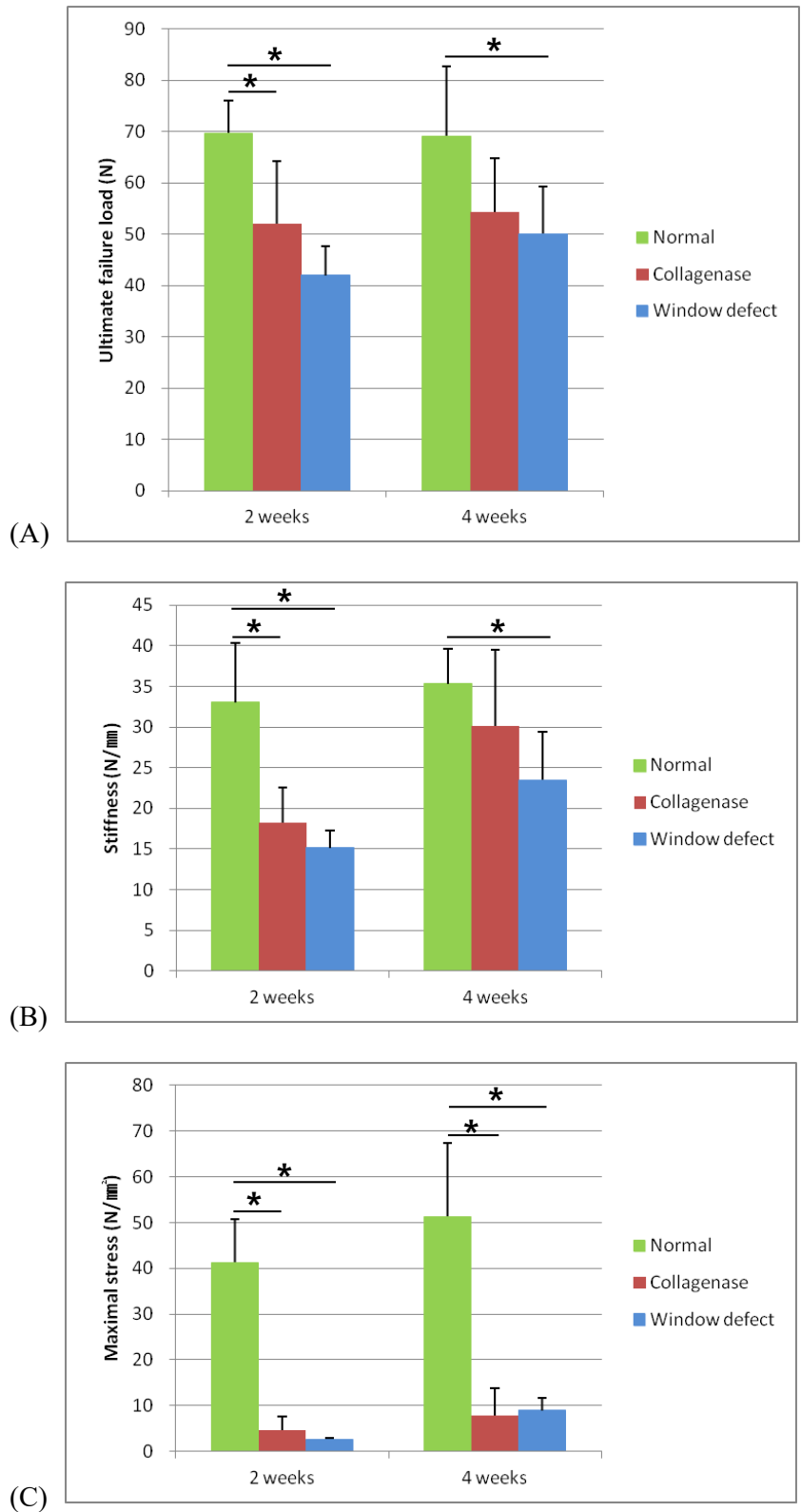


Fig. 4. Biomechanical properties of tendons in each group.

(A) Ultimate failure load, (B) stiffness, and (C) Maximal stress.

* $p < 0.05$ between the normal and collagenase or normal and window defect groups; Mann-Whitney

test.

3. Histological Analysis

Mean total modified Watkins score at 2 weeks was 6.67 ± 0.82 for the collagenase group and 6.17 ± 0.41 for the window defect group. At 4 weeks, the scores were 10.33 ± 1.75 for the collagenase group and 8.17 ± 1.47 for the window defect group. Although the scores were not significantly different between the two groups ($p = 0.31$) at 2 weeks, a significant difference ($p = 0.041$) was found at 4 weeks (Fig. 5). The standard deviation of the window defect group was lower than that of the collagenase group at both time points. The scores for the tendons of the normal control group were all 24. Representative images of each group at each time point are shown (Fig. 6). Chondrocyte-like cells and lacunae were found in all H & E stained slides of both groups at both time points. Representative images for each group are shown (Fig. 7).

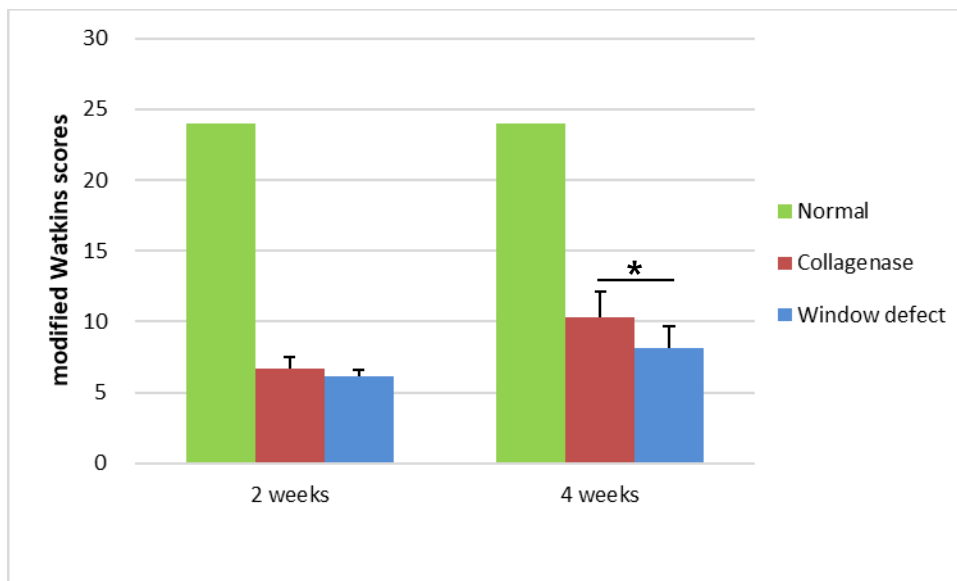


Figure 5. Modified Watkins scores of tendons in each group.

* $p < 0.05$ between the collagenase and window defect groups; Mann-Whitney test.

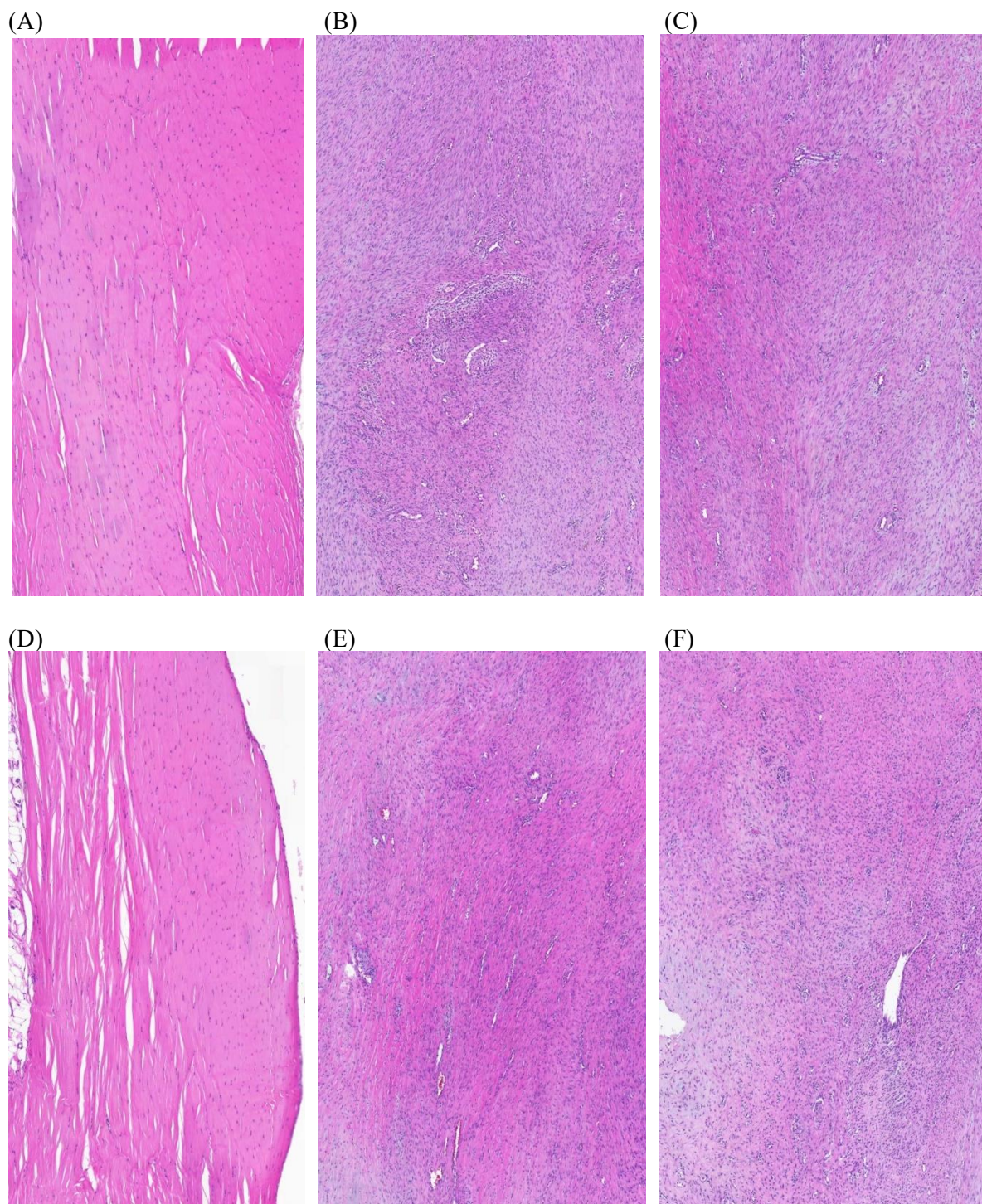


Fig. 6. Hematoxylin and eosin staining

Representative sections of (A) the normal group at week 2 (B) the collagenase group at week 2 (C) the window defect group at week 2 (D) the normal group at week 4 (E) the collagenase group at week 4 (F) and the window defect group at week 4. (magnification 40X). (B) and (C) show marked cellularity, less

than 25% of cells and fibers oriented in parallel, and increased vascularity. (E) and (F) show moderate cellularity, more than 25% of cells and fibers oriented in parallel, and increased vascularity.

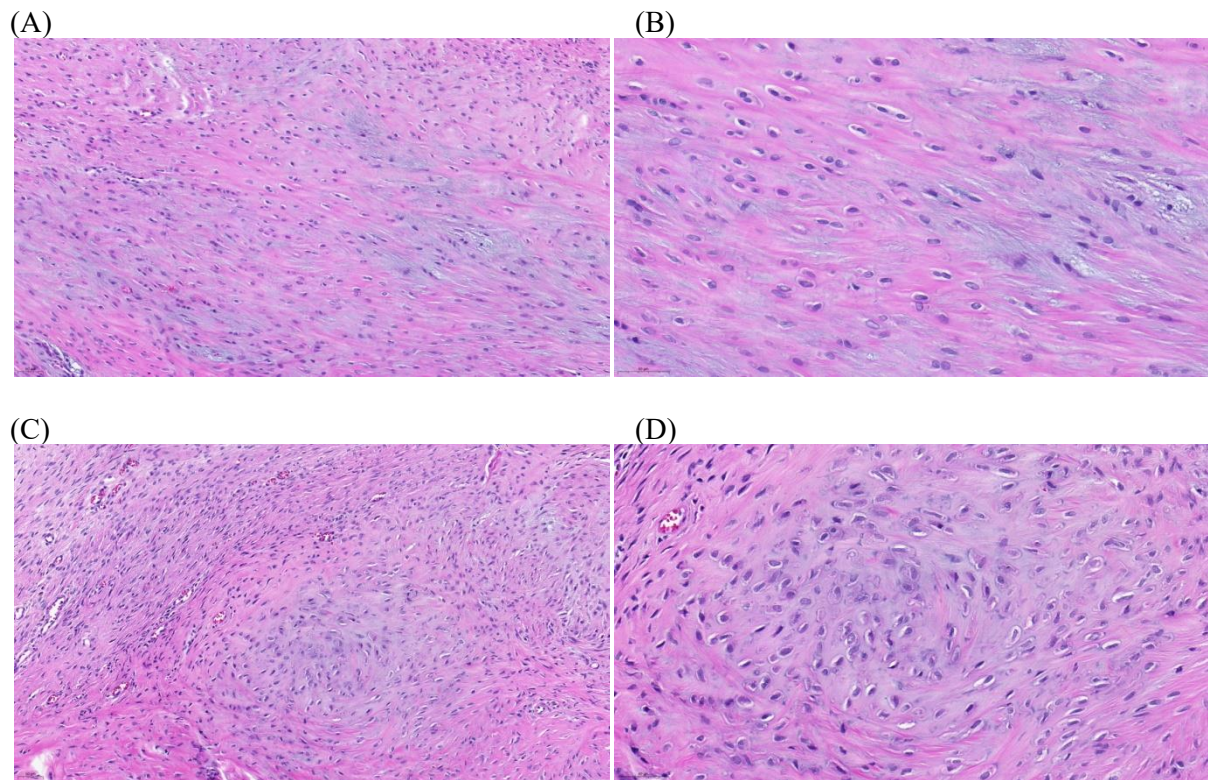


Fig. 7. Representative images of chondrocyte-like cells, lacunae

Hematoxylin and eosin staining of (A, B) the collagenase group at week 4 (C, D) the window defect group at week 4 (magnification, A,C: 200X; B,D: 400X).

4. Immunohistochemistry

The stained area fractions of collagen type I, collagen type III, tenascin C, and BMP 2 did not differ between the collagenase and window defect groups at 2 or 4 weeks (Fig. 8).

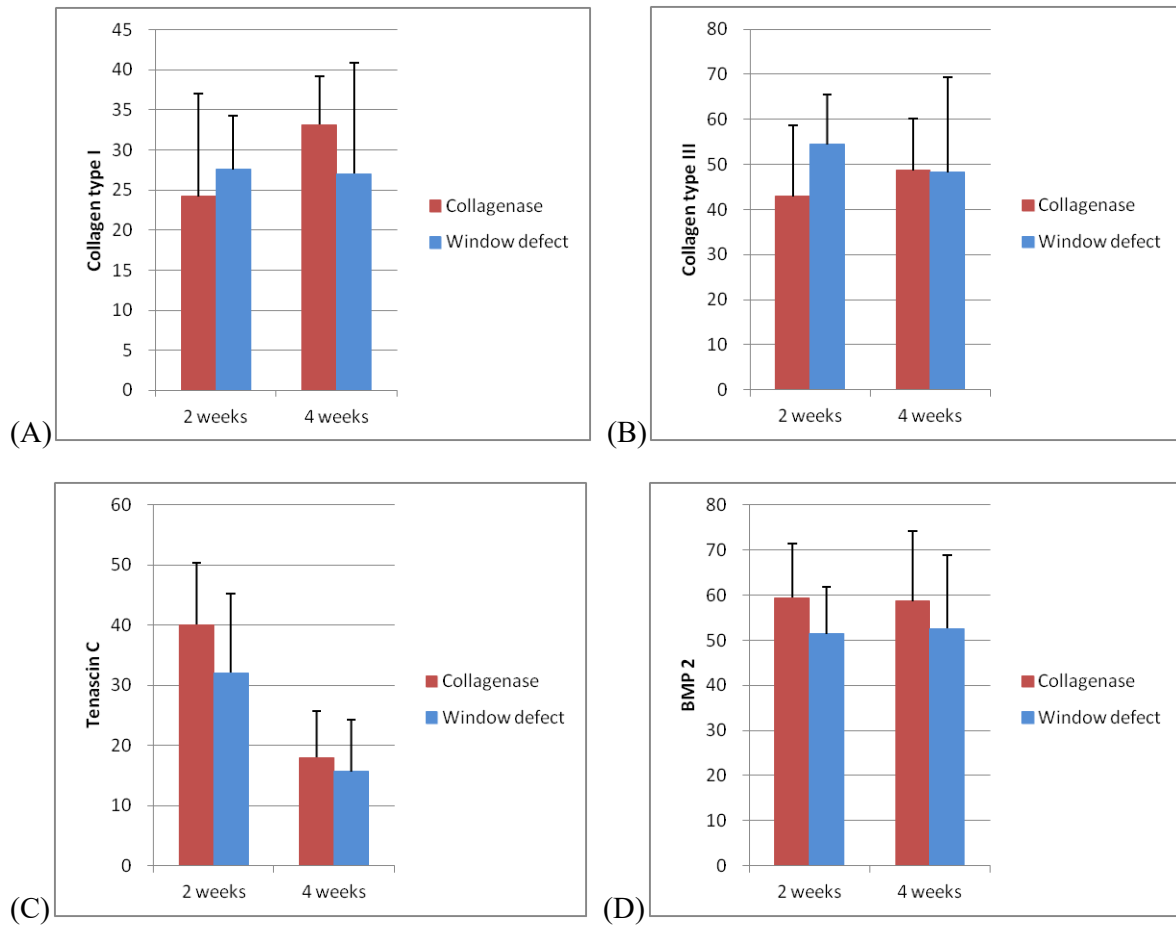


Fig. 8. Quantification of 4 proteins by immunohistochemistry

(A) Collagen type I (B) Collagen type III (C) Tenascin C (D) BMP 2.

* $p < .05$ for difference between collagenase and window defect groups; Mann-Whitney U test.

5. Western Blot Analysis

No significant difference was observed between Collagen type I, collagen type III, tenascin C and BMP 2 protein levels of the collagenase and window defect groups at either 2 or 4 weeks (Fig. 9). Mean protein levels of collagen type III and tenascin C in the window defect group were higher at 2 as well as 4 weeks. Although the BMP 2 level in the collagenase group was higher at 2 weeks, it was higher in the window defect group at 4 weeks. The results for each protein were somewhat different from those for IHC; however, there were no differences in the level of significance.

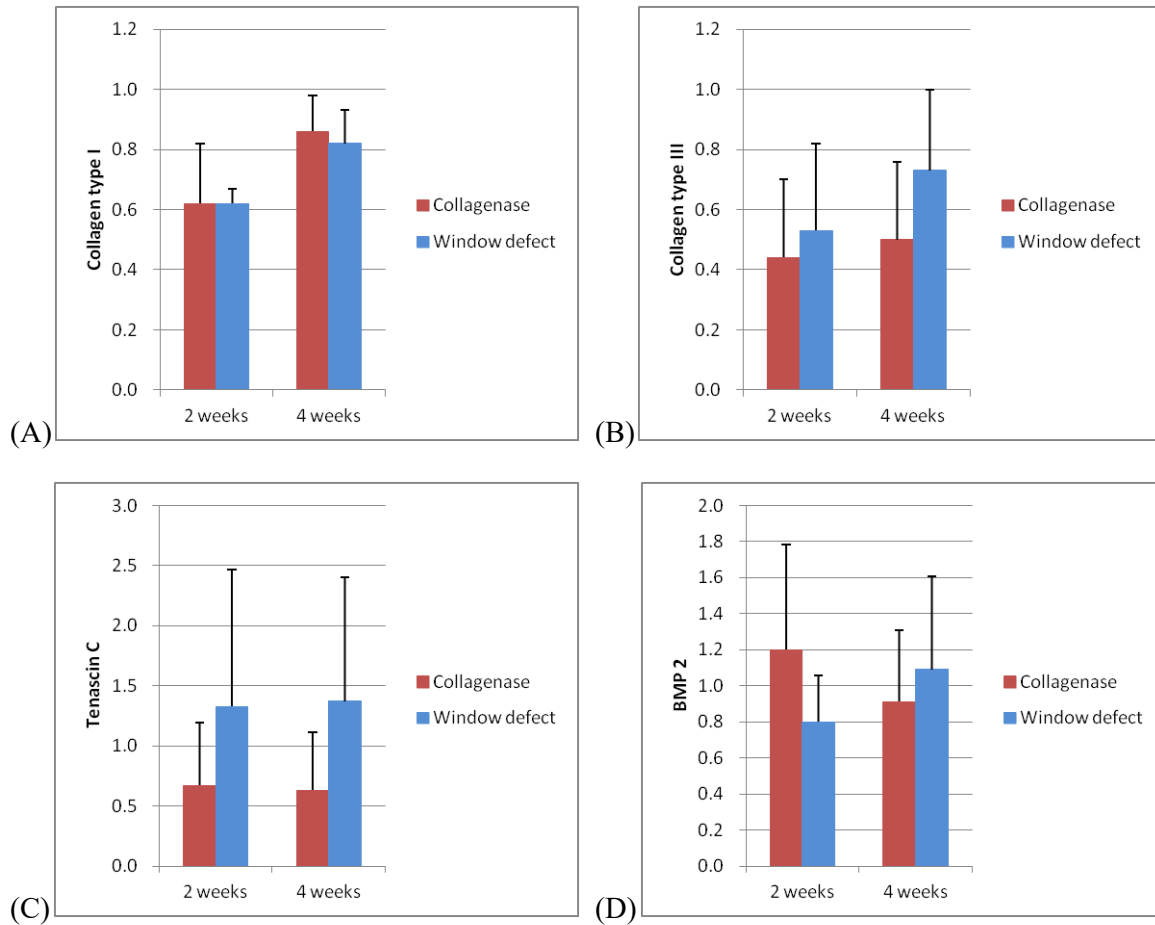


Fig. 9. Quantification of 4 proteins by western blot

(A) Collagen type I (B) Collagen type III (C) Tenascin C (D) BMP 2

* $p < .05$ for difference between collagenase and window defect groups; Mann-Whitney U test.

DISCUSSION

In the present study, I validated rat collagenase-induced and rat window defect-induced Achilles tendon injury models. Based on characteristics of tendinopathy such as CSAs, biomechanical properties and histological parameters, both models appear to be appropriate for use in studies pertaining to tendon injury. The CSAs in both models increased at 2 weeks, but decreased at 4 weeks, whereas biomechanical properties decreased at 2 weeks and increased at 4 weeks, indicating that acute tendon injury was followed by a healing process. Both models displayed diffuse tendinopathy in all H & E stained slides, a feature of a good tendinopathy models. To the best of my knowledge, this is the first study to

comprehensively evaluate histopathological as well as biomechanical aspects of these two injury models for the purposes of comparison.

Although the comparison showed no significant difference between the two models at 2 weeks, some differences were observed in the CSAs and the modified Watkins scores at 4 weeks. The histological score was significantly higher in the collagenase group at 4 weeks, indicating that the window defect group was slower in the tendon repair process. Tendency for slower recovery shown by the window defect model was also reflected in its biomechanical properties. In contrast to the collagenase group, in which ultimate failure load and stiffness were not significantly lower than those of the normal group at 4 weeks, those of the window defect group remained significantly lower than those of the normal group at 4 weeks. However, the CSAs and the protein levels of collagen type III showed inconsistent results in relation to this tendency.

Thickening and increased tendon size are characteristics of tendon injury [26, 27]. A decrease in tendon thickness represents potential improvement in tendinopathy [28]. CSAs of the window defect group showed a greater decline from 2 to 4 weeks than did those of the collagenase group, and became significantly smaller than those of the collagenase group at 4 weeks. This appears to be inconsistent with histological and biomechanical results. However, considering that tendinopathy often coexists with paratendinopathy, which includes edema and hyperemia of the paratenon, CSAs and severity of tendinopathy may not be related in a linear manner [29]. However, the CSA of the window defect group was still four times greater than that of the normal group at 4 weeks.

During the tendon healing process, an initial inflammatory phase, that lasts a few days, is followed by a proliferative phase that lasts for a few weeks [29, 30]. Next, the remodeling phase, during which a higher proportion of collagen type I is synthesized, begins at approximately 6 weeks [31]. Because the synthesis of collagen type III peaks during the proliferative phase, I hypothesized that collagen type III would be expressed more at 2 weeks than at 4 weeks in the faster healing group. Based on the role of

tenascin C in the arrangement of collagen fibrils during tendon regeneration, I expected tenascin C to be expressed more in the faster healing group, [32, 33]. However, IHC and western blot did not indicate any significant intergroup differences between the compositions of collagen type I, collagen type III or tenascin C.

In addition, neither quantitative analyses of BMP 2 via IHC and western blot, nor qualitative evaluations of chondrocyte-like cells, lacunae and calcific deposits via H & E stain slides, indicated a significant intergroup difference. These results were inconsistent with those of a previous study of rat patella tendon injury models. Lui et al., compared BMP 2 expression and calcification between rat collagenase-induced and rat window defect-induced patella tendon injury models, and observed higher levels of BMP 2 at similar chondrogenic and ossification sites in the rat collagenase-induced patella tendon injury model qualitatively [34]. This may be due to differences in the mechanical and material properties between Achilles and patellar tendons [35]. This information may be helpful for researchers who struggle with selecting a rat Achilles tendon injury model when investigating calcific tendinitis at the Achilles tendon.

Based on the fact that the results of the current study did not indicate any remarkable differences between these two models, researchers may consider methodological problems. The collagenase-induced model requires less time and resources than the window defect model [2]. In addition, the collagenase-induced model may be less stressful for the experimental animals. However, if a study requires experimental injections to be administered several times following the induction of a tendon injury and needs space for this purpose, using the window defect model would be more convenient. A researcher may easily decide on the type of rat Achilles tendon injury model needed for a study, according to the circumstances affecting his or her study.

The present study was beset by several limitations. First, because the acute injury model was evaluated using young rats, direct clinical application was limited. Secondly, the long term progression of these injury models was not evaluated for more than 4 weeks. Because the regenerative process of a tendon

lasts longer than 4 weeks, several differences that materialized later than 4 weeks may have been missed by the current study. Thirdly, the tenascin C features seen in the results of IHC and western blot were somewhat different. It is desirable that the trends displayed by IHC and western blot are in proportion. Though there were no significant differences between the two studies that affected the results, these technical issues should be given due consideration.

CONCLUSION

Both rat collagenase-induced and rat window defect-induced Achilles tendon injury models are appropriate for use in studies investigating tendon injuries. Both models reflect the clinical, biomechanical, and histological characteristics of tendinopathy well. Although no great differences were observed between these two models, the window defect model displayed a tendency towards slower recovery. This study imparts helpful information that may enable to researchers who are in the process of designing animal studies, to decide between rat collagenase-induced and rat window defect-induced Achilles tendon injury models.

REFERENCES

1. Cardoso, T.B., et al., *Current trends in tendinopathy management*. Best Pract Res Clin Rheumatol. 2019. **33**(1):p. 122-140.
2. Hast, M.W., A. Zuskov, and L.J. Soslowsky, *The role of animal models in tendon research*. Bone Joint Res, 2014. **3**(6): p. 193-202.
3. Huegel, J., et al., *Quantitative comparison of three rat models of Achilles tendon injury: A multidisciplinary approach*. J Biomech, 2019. **88**: p. 194-200.
4. Chen, L., et al., *Tendon derived stem cells promote platelet-rich plasma healing in collagenase-induced rat achilles tendinopathy*. Cell Physiol Biochem, 2014. **34**(6): p. 2153-68.
5. Huang, T.F., et al., *Mesenchymal stem cells from a hypoxic culture improve and engraft Achilles tendon repair*. Am J Sports Med, 2013. **41**(5): p. 1117-25.
6. Lee, S.Y., et al., *Therapeutic Mechanisms of Human Adipose-Derived Mesenchymal Stem Cells*

- in a Rat Tendon Injury Model*. Am J Sports Med, 2017. **45**(6): p. 1429-1439.
7. Okamoto, N., et al., *Treating Achilles tendon rupture in rats with bone-marrow-cell transplantation therapy*. J Bone Joint Surg Am, 2010. **92**(17): p. 2776-84.
 8. Oshita, T., et al., *Adipose-Derived Stem Cells Improve Collagenase-Induced Tendinopathy in a Rat Model*. Am J Sports Med, 2016. **44**(8): p. 1983-9.
 9. Riley, G., *The pathogenesis of tendinopathy. A molecular perspective*. Rheumatology (Oxford), 2004. **43**(2): p. 131-42.
 10. Marsolais, D., C.H. Côté, and J. Frenette, *Neutrophils and macrophages accumulate sequentially following Achilles tendon injury*. J Orthop Res, 2001. **19**(6): p. 1203-9.
 11. Wetzel, B.J., et al., *Quantitative characterization of rat tendinitis to evaluate the efficacy of therapeutic interventions*. Biomed Sci Instrum, 2002. **38**: p. 157-62.
 12. Machova Urdzikova, L., et al., *Human multipotent mesenchymal stem cells improve healing after collagenase tendon injury in the rat*. Biomed Eng Online, 2014. **13**: p. 42.
 13. Yang, Z., et al., *Effect of Tendon Stem Cells in Chitosan/ β -Glycerophosphate/Collagen Hydrogel on Achilles Tendon Healing in a Rat Model*. Med Sci Monit, 2017. **23**: p. 4633-4643.
 14. Ni, M., et al., *Tendon-derived stem cells (TDSCs) promote tendon repair in a rat patellar tendon window defect model*. J Orthop Res, 2012. **30**(4): p. 613-9.
 15. Xu, K., et al., *Synergistic promoting effects of bone morphogenetic protein 12/connective tissue growth factor on functional differentiation of tendon derived stem cells and patellar tendon window defect regeneration*. J Biomech, 2018. **66**: p. 95-102.
 16. Xu, W., et al., *Human iPSC-derived neural crest stem cells promote tendon repair in a rat patellar tendon window defect model*. Tissue Eng Part A, 2013. **19**(21-22): p. 2439-51.
 17. Messner, K., et al., *Rat model of Achilles tendon disorder. A pilot study*. Cells Tissues Organs, 1999. **165**(1): p. 30-9.
 18. Sullo, A., et al., *The effects of prolonged peritendinous administration of PGE1 to the rat Achilles tendon: a possible animal model of chronic Achilles tendinopathy*. J Orthop Sci, 2001. **6**(4): p. 349-57.

19. Perucca Orfei, C., et al., *Dose-Related and Time-Dependent Development of Collagenase-Induced Tendinopathy in Rats*. PLoS One, 2016. **11**(8): p. e0161590.
20. Warden, S.J., *Animal models for the study of tendinopathy*. Br J Sports Med, 2007. **41**(4): p. 232-40.
21. Brown, T.D., F.H. Fu, and E.N. Hanley, Jr., *Comparative assessment of the early mechanical integrity of repaired tendon Achilles ruptures in the rabbit*. J Trauma, 1981. **21**(11): p. 951-7.
22. Noguchi, M., et al., *A method of in-vitro measurement of the cross-sectional area of soft tissues, using ultrasonography*. J Orthop Sci, 2002. **7**(2): p. 247-51.
23. Kraus, T.M., et al., *Stem cells and basic fibroblast growth factor failed to improve tendon healing: an in vivo study using lentiviral gene transfer in a rat model*. J Bone Joint Surg Am, 2014. **96**(9): p. 761-9.
24. Ide, J., et al., *The effects of fibroblast growth factor-2 on rotator cuff reconstruction with acellular dermal matrix grafts*. Arthroscopy, 2009. **25**(6): p. 608-16.
25. Yokoya, S., et al., *Tendon-bone insertion repair and regeneration using polyglycolic acid sheet in the rabbit rotator cuff injury model*. Am J Sports Med, 2008. **36**(7): p. 1298-309.
26. Khan, K.M., et al., *Histopathology of common tendinopathies. Update and implications for clinical management*. Sports Med, 1999. **27**(6): p. 393-408.
27. Krogh, T.P., et al., *Ultrasonographic assessment of tendon thickness, Doppler activity and bony spurs of the elbow in patients with lateral epicondylitis and healthy subjects: a reliability and agreement study*. Ultraschall Med, 2013. **34**(5): p. 468-74.
28. Zhang, Y.J., et al., *Is Platelet-rich Plasma Injection Effective for Chronic Achilles Tendinopathy? A Meta-analysis*. Clin Orthop Relat Res, 2018. **476**(8): p. 1633-1641.
29. Sharma, P. and N. Maffulli, *Tendon injury and tendinopathy: healing and repair*. J Bone Joint Surg Am, 2005. **87**(1): p. 187-202.
30. Oakes, B.W., *Tissue Healing and Repair: Tendons and Ligaments*, in *Rehabilitation of Sports Injuries: Scientific Basis*, W.R. Frontera, Editor. 2003, Blackwell Science: Boston. p. 56-98.
31. Abrahamsson, S.O., *Matrix metabolism and healing in the flexor tendon. Experimental studies*

- on rabbit tendon*. Scand J Plast Reconstr Surg Hand Surg Suppl, 1991. **23**: p. 1-51.
32. Reed, S.A. and S.E. Johnson, *Expression of scleraxis and tenascin C in equine adipose and umbilical cord blood derived stem cells is dependent upon substrata and FGF supplementation*. Cytotechnology, 2014. **66**(1): p. 27-35.
 33. Veronesi, F., et al., *Effect of adipose-derived mesenchymal stromal cells on tendon healing in aging and estrogen deficiency: an in vitro co-culture model*. Cytotherapy, 2015. **17**(11): p. 1536-44.
 34. Lui, P.P., et al., *Expression of bone morphogenetic protein-2 in the chondrogenic and ossifying sites of calcific tendinopathy and traumatic tendon injury rat models*. J Orthop Surg Res, 2009. **4**: p. 27.
 35. Obst, S.J., *Are the Mechanical or Material Properties of the Achilles and Patellar Tendons Altered in Tendinopathy? A Systematic Review with Meta-analysis*. Sports Med. 2018. **48**(9): p. 2179-2198.

백서 아킬레스건의 콜라겐분해효소(collagenase) 유도 손상 모델과

창형손상(window defect) 모델의 검증 및 비교

목적 동물 실험을 포함한 힘줄 연구에서 적절한 동물 모델을 선택하는 것은 중요하다. 본 연구는 백서 아킬레스건의 콜라겐분해효소(collagenase) 유도 손상 모델과 창형손상(window defect) 모델의 적절성을 각각 검증하고, 두 모델을 비교해 보고자 하였다.

방법 27마리의 10주령 백서에서 총 54개의 아킬레스건을 얻어, (1) 콜라겐분해효소군 (2) 창형손상군 (3) 정상군의 3군으로 18개씩 임의 배정하였다. 콜라겐분해효소군은 아킬레스건에 10 μ l의 제 1형 콜라겐분해효소를 2회 주사하였고, 창형손상군은 종골 접착부로부터 폭 0.6mm, 길이 6mm의 창형 절제 부위를 만들었다. 모델 형성 후 2주 및 4주가 지난 시점에 힘줄의 단면적, 생역학적, 조직학적, 면역조직화학 평가를 시행하고, 웨스턴블롯 검사도 시행하였다.

결과 힘줄 단면적은 2주와 4주 모두에서 콜라겐분해효소군과 창형손상군이 모두 정상군에 비해 유의하게 컸다. 두 모델군 비교 시 4주에는 콜라겐분해효소군이 창형손상군에 비해 단면적이 유의하게 컸다. 2주 시점에는 최종 파열력, 강성, 최대 스트레스 수치가 두 모델군이 정상군에 비해 유의하게 낮았고, 4주 시점에 회복되며 증가하였다. 콜라겐분해효소군은 4주 시점에 최종 파열력과 강성이 더 이상 정상군보다 유의하게 낮지 않았다. 조직학적 평가에서 두 모델군 모두에 전반적인 힘줄병증의 특징이 나타났고, 모든 조직 슬라이드에서 연골세포양 세포들과 열공이 관찰되었다. 수정된 왓킨 점수는 4주 시점에는 창형손상군이 콜라겐분해효소군보다 유의하게 낮았다. 두 모델군의 면역조직화학 평가 및 웨스턴블롯 검사로 확인한 콜라겐 I 형, 콜라겐 III 형, 테나신 C, BMP 2 단백질의 양은 두 모델군에서 모두 유의한 차이를 보이지 않았다.

결론 본 연구를 통해 백서 아킬레스건의 콜라겐분해효소 유도 손상과 창형손상 모델은 모두 힘줄 손상 연구에 사용하기 적합하다는 것을 검증하였다. 두 모델 비교 시 둘 간에 큰 차이는 없었으나 창형손상 모델의 재생 속도가 더딘 경향을 보였다.